ELSEVIER

Food Chemistry 70 (2000) 499–508

Food Chemistry

www.elsevier.com/locate/foodchem

Analytical, Nutritional and Clinical Methods Section

Oxygen permeation through an oil-encapsulating glassy food matrix studied by ESR line broadening using a nitroxyl spin probe

Astrid B. Andersen, Jens Risbo, Mogens L. Andersen, Leif H. Skibsted *

Food Chemistry, Department of Dairy and Food Science, Royal Veterinary and Agricultural University, Rolighedsvej 30, DK-1958 Frederiksberg C, Denmark

Received 18 October 1999; received in revised form 31 January 2000; accepted 31 January 2000

Abstract

A non-invasive method based on the broadening of electron spin resonance (ESR) lines in the presence of oxygen (oximetry) has been developed to determine the rate of permeation of oxygen from head space into oil, encapsulated in a glassy matrix (a food model made from sucrose, maltodextrin and gelatine by freeze-drying). The lipophilic nitroxide 16-doxylstearic acid, 16-DSA, was used as a spin-probe, and it was found to be concentrated mainly in the oil phase in the glassy matrix. The concentrations of oxygen in the freshly made glasses were found to be similar to the concentration in atmospheric air, and the process of freeze-drying is apparently not able to remove oxygen before the glassy system solidifies. Storing the oil-encapsulating glasses under oxygen increased the oxygen concentration inside the matrices, and the rate of permeation was found to increase with temperature. A kinetic model for the oxygen permeation was established, based on the rate data obtained up to full saturation of the oil with oxygen below the glass transition temperature ($T_g = 65°C$), and on data for partial oxygen saturation above the glass transition temperature. The kinetic model includes a temperature independent master curve and allows for structural heterogeneity. The energy of activation for oxygen permeation was found to be 74 ± 6 kJ/mol for the glassy matrix, and the large value is in favour of the molecular model for oxygen diffusion rather than the free volume model, and accords with the zeroth-order kinetics for oxidation of lipids encapsulated in a glassy matrix, which has previously been observed to be associated with oxygen permeation as the rate-determining step.

1. Introduction

Foods with high concentrations of carbohydrates or proteins are often able to form a glassy phase upon drying or freezing, and lipids present may become encapsulated as in dried whole egg powder, milk powder, and instant soups. An increased long term stability of the food system is often associated with the glassy state and this effect has generally been rationalized as a consequence of the high viscosity (Sun, Leopold, Crowe & Crowe, 1996).

The permeability of oxygen through the glassy matrix in food systems is of outmost importance for the storage stability of encapsulated oils and for the viability of freeze-dried starter cultures (Andersen, Fog-Petersen, Larsen & Skibsted, 1999). Oxygen permeability coefficients have been measured for glassy carbohydrate systems with simple geometries such as films (Arvantioyannis, Kalichevsky & Blanshard, 1994), whereas studies of oxygen permeation in food model systems are of a more indirect nature. Imagi, Muraya, Yamahita, Adachi and Matsuno (1992) estimated the diffusion coefficient of oxygen dissolved in glassy matrices of sugar or protein to be in the range of 10^{-2} m^2/s from an estimate of lipid oxidation. It has also been reported that encapsulated lipids are not oxidized unless the glassy matrix crystallizes or collapses (Labrousse, Roos & Karel, 1992).

ESR oximetry has proved to be a powerful technique for measuring oxygen concentrations inside biological systems (Swartz & Glockner, 1989). The method relies on incorporating a paramagnetic substance, a spin probe, into the biological sample. Oxygen, which itself is

* Corresponding author. Tel.: +45-3528-3221; fax: +45-3528-3344.

E-mail address: ls@kvl.dk (L.H. Skibsted).

0308-8146/00/$ - see front matter
PII: S0308-8146(00)00102-3

a paramagnetic substance, broadens the ESR signal of the spin probe through Heisenberg spin exchange in such way that a change in line width, Δw, is linearly proportional to the oxygen concentration (Swartz & Glockner, 1989).

Paramagnetic coal based materials, lithium phthalocyanine, and nitroxyl radicals have been used as spin probes for ESR oximetry (Afeworki, Miller, Devashahayam, Cook, Mitchell, Subramanian & Krishna, 1998; Inoue, Utsumi & Kirino, 1994). Nitroxyl radicals have the advantage of responding almost instantaneously to changes in oxygen concentration, corresponding to the rate of a bimolecular collision. Furthermore, the nitroxide group can be attached to a wide range of host molecules for design of spin probes with specific properties (Morse & Smirnov, 1995).

In this paper we present results from a continuation of the work of Orlien, Andersen, Sinkko and Skibsted (2000) on a food model of vegetable oil encapsulated in a glassy matrix made from sucrose, maltodextrin and gelatine, for which permeation of oxygen through the matrix was found to be rate-limiting for oxidation of encapsulated oil. In the present work we address the question of oxygen permeation in a more direct way, and monitor the oxygen concentration of encapsulated oil as a function of time and temperature on both sides of the glass transition temperature by using ESR oximetry with a lipophilic nitroxide spin probe located in a saturated, non-oxidizable oil as the encapsulated phase.

2. Materials and methods

2.1. Preparation of emulsions and storage

Solutions were made of 2.25 g sucrose (extra pure, Merck, Darmstadt, Germany), 1.25 g maltodextrin (DE 10, from maize starch, Fluka, Neu-Ulm, Switzerland) and 0.25 g gelatine (225 bloom, from calf skin, Aldrich, Milwaukee, USA) in 24 ml water (MilliQ, Millipore Q-plus, Millipore Corporation, Ma, USA). The solutions were emulsified with 1.25 g saturated Medium Chain Triglyceride oil (MCT-oil, Delios® V, Grünau Illertissen Gmbh, Illertissen, Germany) made 0.217 mM with the spin probe 16-doxylstearic acid (16-DSA, Aldrich, Milwaukee, USA) for 5 min with a homogeniser (Ultra Turrax, Jankel & Kunkel IKA-Labortechnich, Staufed, Germany). The samples were frozen in a 1 cm layer at −80°C and freeze-dried ($P = 0.1$ mbar, 48 h). The freeze-dried material was transferred to ESR tubes that were open at both ends (clear fused quartz, inner diameter 4 mm, outer diameter 5 mm, length 180 mm, Wilmad Glass Co., Buena, NJ, USA), and the tubes were closed at one end with a plug of glass wool. Non-encapsulated oil was removed by washing three times with hexane (HPLC-grade, Fisher Scientific, Leicestershire, UK) in the ESR tubes and the material was dried for one week in an evacuated desiccator over P_2O_5 at room temperature.

The ESR tubes were transferred to 500 ml separation funnels with glass taps at both ends functioning as desiccators. Each desiccator contained three ESR tubes with freeze dried and washed food model, a small paper bag of silica gel, an ESR tube with 0.217 mM 16-DSA in MCT oil and a sample of the food model for DSC and water content measurements. The desiccators were flushed with 100% O_2 or 100% N_2 for 10 min immediately after each measurement to reestablish the atmosphere. Desiccators flushed with 100% O_2 were stored at 5, 22, 37, 45, 60, 65, 70, 75 and 80°C, and the desiccator that was flushed with 100% N_2 was stored at 22°C. The experiment was repeated for samples stored at 22°C.

2.2. Electron spin resonance measurements

ESR spectra were recorded with a Jeol FR30 spectrometer (Jeol, Tokyo, Japan). Typical instrument parameters used were microwave power: 4 mW, sweep width: 7.5 mT, sweep time: 4 min, modulation width: 0.1 mT, and time constant: 0.3 s. The spectra were analysed in terms of the peak to peak line width, ΔH_{pp}, of the central line ($M_I = 0$) (cf. Fig. 2 below), and the amount of spin probe was quantified as the area obtained by integrating the derivative ESR spectra twice.

Standard curves of ΔH_{pp} against the oxygen concentration were obtained by saturating a solution of 43.4 μM 16-DSA in MCT oil with gas mixtures (Hede Nielsen A/S, Tåstrup, Denmark) of oxygen and nitrogen (0, 21, 40, 60, 80 and 100% vol. O_2) immediately before recording the ESR spectra. Standard curves were obtained at each temperature by equilibrating the oil with the gas mixtures at 5, 22, 37, 45, 60, 70 and 80°C, respectively, and sealing the ESR tubes. All ESR spectra were recorded at 22°C.

ESR spectra of the food models were recorded at given intervals during a period of 48 days. The ESR tubes containing the food models stored in an oxygen atmosphere were gently flushed with oxygen during the measurements, and the food models stored under nitrogen were flushed with nitrogen. Every second set of the regular ESR measurements was supplemented with additional experiments in order to examine the amount of poorly or non-encapsulated 16-DSA-containing oil not removed by washing and accessible to oxygen or nitrogen within a short timescale. The additional ESR measurements were performed by gently flushing the samples with nitrogen and oxygen for food models stored under oxygen and nitrogen atmospheres, respectively, for 10 min before recording the ESR spectra. The amount of non-encapsulated oil was, furthermore, examined on the final day of the experiment by washing the food models thoroughly with hexane, and compar-

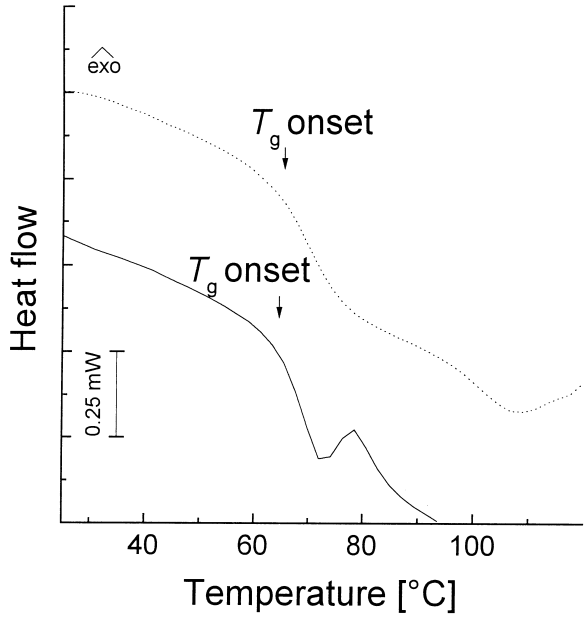

Fig. 1. DSC scan of food model heated from 20 to 90°C with 5°C/min (——), cooled and reheated from 20 to 120°C with 5°C/min (·····). The glass transition temperature (T_g) is taken as the onset of the step change in heat flow.

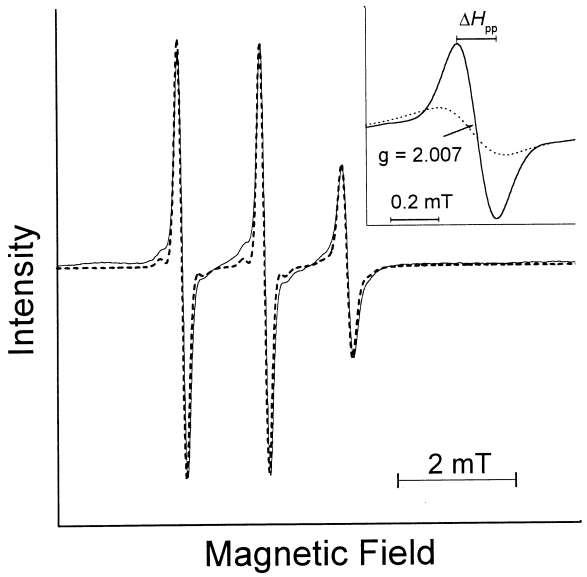

Fig. 2. Comparison of ESR spectra of 0.217 mM 16-DSA in encapsulated oil (——) and bulk oil (----) at 100% N_2. Curves are normalized by the intensity of centre line. Inset shows centre line spectra of food model system at day 0 (——) and at day 33 (·····) of storage at 60°C in a 100% oxygen atmosphere. Curves in inset are normalised by the amount of probe.

ing the intensities of ESR spectra recorded before and after this second hexane-washing.

2.3. Water content

Water content of the food models was recorded by Karl Fischer titration (Mettler Toledo DL18, Schwerzenbach, Switzerland). Samples (0.2 g) were incubated with 6 ml water-free methanol (0.001% H_20, BHT, Laboratory Suppl., Poole, England) for 24 h at room temperature for extraction of water. Aliquots of 1 ml of the extract were titrated.

2.4. Differential scanning calorimetry

The glass transition temperature, T_g, of the food model was determined using a DSC 820 from Mettler Toledo (Schwerzenbach, Switzerland). The DSC 820 is based on the heat flux principle and cooled with liquid nitrogen. Calibrations of heat flow and temperature were performed with indium (mp = 156.6°C, $\Delta_{fus}H = 28.5$ J/g), zinc (mp = 419.5°C, $\Delta_{fus}H = 107.5$ J/g), gallium (mp = 29.8 C, $\Delta_{fus}H = 80.1$ J/g) and *n*-decane (mp = −29.7°C, $\Delta_{fus}H = 202.1$ J/g) as standards. Five to 15 mg of food model was hermetically sealed into 40 μl aluminium DSC crucibles (ME 27331). An empty sealed aluminium crucible was used as reference . The samples were taken through a temperature course from 10 to 95 to 10 to 120°C with 5°C/min. Triplicates and rescans verified, in each case, the endothermic baseline shift associated with a glass transition. The glass transition temperature T_g was taken as the onset of the endothermic baseline shift.

2.5. Oxidative stability

The oxidative stability of the MCT oil was investigated by measuring the peroxide value of samples stored at 5, 22, 37 and 45°C after storage for 48 days by the IDF Standard 74A (1991).

2.6. Non-linear curve fitting

Non-linear curve fitting was performed using the Origin graphical software package (Microcal Software, Inc., Northhampton, MA, USA).

3. Results

3.1. The food model

The food model was a slightly modified version of the system previously designed to be stable against crystallization and collapse and characterized by optical and scanning electron microscopy (Orlien et al., 2000). The glassy matrix encapsulating the oil had a fragile and porous structure, and the oil particles were found to have sizes in the order of 20 μm and to be encapsulated and distributed throughout the matrix. The food model used in the present study was modified by using an oxidatively stable MCT oil consisting of mixed decanoyl

and octanoyl triglycerides, in contrast to the previous study in which rapeseed oil, had azo-compounds added in order to initiate oxidation. The spin probe 16-DSA was incorporated into the food model by dissolving it in the MCT oil prior to emulsification.

The glass transition temperature and the water content of the food models were measured for each storage temperature after 40 days of storage. The temperature program of the DSC measurements was designed to heat the sample to a temperature just above the assumed glass transition and cool again before reheating the sample. In this way it was verified that the observed base line shift was reversible, giving a strong indication of a glass transition, as seen in Fig. 1. The glass transition temperature was $T_g = 64.7 \pm 2.1$°C and the water content was 1.0 ± 0.7%, independent of the storage temperature.

3.2. 16-DSA as an ESR oximetric spin probe in neat oil and in the food model

ESR spectra of the food model containing 16-DSA were three-line ESR spectra that were similar to the spectrum of a solution of 16-DSA in MCT-oil as shown in Fig. 2. The close similarity between the ESR spectra of the two systems suggests that the mobility of 16-DSA is identical in the two systems, and 16-DSA is most likely found mainly in the oil-droplets of the food model. However, a small contribution of a nitroxyl radical powder spectrum can be seen in the ESR spectrum of the food model. This is most likely arising from some of the 16-DSA molecules that have been immobilized by being trapped in the glassy matrix or at the oil/glass surface. Storing the 16-DSA-containing food model under oxygen led to a broadening of the ESR lines. An example is shown in the insert of Fig. 2, where the signals have been normalised with respect to the doubly integrated area.The central line of the spectrum of a sample is shown after 0 and 33 days of storage under 100% oxygen at 60°C. An increase in the line width, ΔH_{pp}, was observed after the storage under oxygen, together with a decrease in the intensity of the signals.

The line shape of nitroxyl radicals consists of an envelope of Lorentzian lines which is a result of the hyperfine splitting caused by the interaction of the spin of the nitroxyl moiety with the neighbouring protons. The broadening, Δw, of each of the Lorentzian lines is expected to depend linearly on the oxygen concentration. However, a similar dependence is not assured for the line width, ΔH_{pp}, of the composite ESR line of the nitroxyl spin probe (Swartz & Glockner, 1989). A standard curve of ΔH_{pp} was, therefore, constructed by recording ESR spectra of a solution of 16-DSA in oil that had been equilibrated with different mixtures of nitrogen and oxygen. A plot of ΔH_{pp} versus the oxygen content of the gas mixtures gave a straight line as shown in Fig. 3A. The line width increased from 0.14 mT to 0.28 as the oxygen content of the gas mixture was increased from 0 to 100%. Within the experimental accuracy, no temperature dependency of ΔH_{pp} could be detected, implying that changes in oxygen solubility with temperature were too small to be measured. The 16-DSA concentration in the bulk oil was varied from 0.217 to 0.0050 mM and the line width recorded; however, no change in line width was observed, indicating that the contribution of spin exchange between 16-DSA molecules to the overall broadening of the ESR lines is

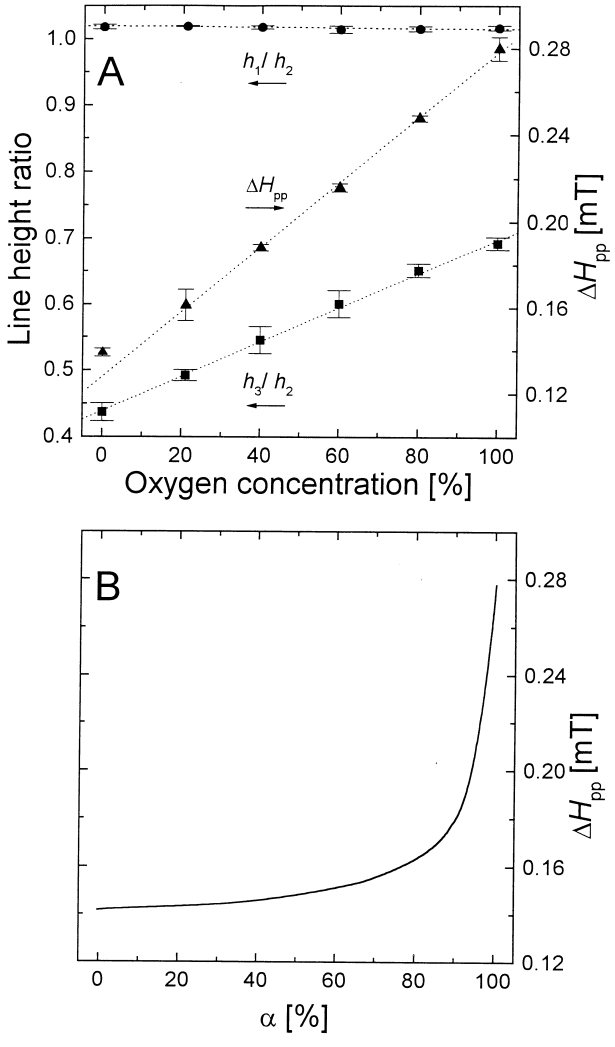

Fig. 3. Standard curves of spectral properties as a function of atmospheric oxygen concentration. (A) Centre line width (▲) of 43.4 μM 16-DSA in bulk oil as a function of gas phase oxygen concentration (%) as an average from bulk oils being purged with gas mixtures at 5, 22, 37, 45, 60, 70 and 80°C and recorded at 22°C. Ratio of line heights; (■) third line over centre line (h_3/h_2), (●) first line over centre line (h_1/h_2). Lines represent linear fit of standard curve from 21 to 100% O_2 in each case. (B) Line width, ΔH_{pp}, as a function of volume fraction, α, for observed spectra, $F_{obs}(B)$ [cf. Eq. (1)], for a heterogeneous two-compartment system.

negligible in this range of concentrations of 16-DSA in oil. It was also found that the ratio of line heights of the high field line,h_3, and the central line, h_2, was linear with the concentration of oxygen, whereas the ratio of the heights of the low field line and the central line h_2/h_1 was constant (Fig. 3A). Recording the ratio h_3/h_2 can therefore be regarded as an alternative method for measuring oxygen concentrations.

It should be emphasised that the standard curve, Fig. 3A, was obtained by using a homogeneous oil system, whereas the food model is an inhomogeneous system where the barrier properties of the glassy matrix can maintain gradients in oxygen concentration over long periods. The observed ESR spectrum of the present system is made up of a sum of ESR-spectra with differing line widths, and the line width of the resulting spectrum is a function of the distribution of size and oxygen concentration of the oil particles. The effect of such inhomogeneities on the observed line width, $\Delta H_{pp,}$ was studied by simulating the ESR spectra of a simple two-compartment system containing MCT oil with 43.4 μM 16-DSA. In one compartment, a volume fraction, α, of the oil is equilibrated with 100% oxygen and, in the other compartment, a volume fraction, 1-α, is equilibrated with nitrogen. In the case where the nitroxide probes are not able to exchange between the two compartments, the observed spectrum $F_{obs}(B)$ is the weighted sum of the spectra of each compartment:

$$F_{obs}(B) = \alpha F_{o2}(B) + (1-\alpha)F_{N2}(B), \quad (1)$$

where $F_{O2}(B)$ and $F_{N2}(B)$ are measured spectra of the standard curve, which are normalized with respect to the amount of probe. The line width, ΔH_{pp}, of the resulting spectrum $F_{obs}(B)$ is shown as a function of the fraction α in Fig. 3B. It should be noted that α can be interpreted as the simple average oxygen concentration of the two-compartment system, allowing a direct comparison between Fig. 3A and B. When α is decreased from 100 to 80% a large decrease of about 0.12 mT is observed in ΔH_{pp}, whereas the corresponding increase in α from 0 to 20% only results in a small increase of about 0.01 mT. The non-linearity of the ΔH_{pp} (α) curve implies that a small part of a heterogeneous system with a low concentration of oxygen can dominate the observed line width due to the sharpness and high intensity of the ESR spectrum of this part of the system as compared to the broadened and less intense spectrum of the rest of the system. For a more realistic multi-compartment system, as the food model under study, the practical implications should be a more cautious use of the linear standard, Fig. 3A. A straightforward interpretation of a measured ΔH_{pp} by the use of Fig. 3A does not give the simple average oxygen concentration, but rather an average concentration where the oxygen-poor regions are given higher weightings. In that sense, the oxygen concentrations estimated from Fig. 3A should be regarded as a lower boundary for the true average concentration.

3.3. Stability of the spin probes in the food model

The stability of the 16-DSA spin probe during the storage of the food model at elevated temperatures for long periods of time was examined by comparing the amounts of spin probe in the samples quantified as the doubly-integrated areas of the ESR spectra. It was found that 94 ± 4% of the spin probe remained in the food model after 25 days of storage at temperatures in the range from 5 to 60°C. At temperatures above T_g, the probe decayed more rapidly. Thus, at 70, 75 and 80°C only 79, 65 and 57%, respectively, remained after 25 days of storage. The shape of the spectrum did not change, despite the relatively high degree of decay of the spin probe during the long time of storage at these high temperatures, as can be seen from Fig. 4A, where the intensities of the central ESR lines have been normalised in order to facilitate comparison.

The ESR spectra of food models after 33 days of storage at a high temperature (75°C) and a low temperature (5°C) under a 100% oxygen atmosphere are compared in Fig. 4B (the intensities of the central line have been adjusted to be equal). The ESR lines of the sample stored at 75°C are broadened when compared to the sample stored at 5°C, which indicates that oxygen has been able to penetrate the glassy matrix at the high temperature of storage. The difference in the heights of the high field lines of the two samples can be explained as a result of the difference in oxygen penetration (vide supra). Since the differences between the two spectra can be completely explained as a result of the different degrees of oxygen permeation into the oil phase in the two samples, the possibility that the surroundings of the 16-DSA spin probe should be different in the two systems, and that difference in probe degradation influences the measurement, can accordingly be eliminated.

3.4. Oxygen permeation in food model

Fig. 5 shows the time courses of the line width, ΔH_{pp}, for food models exposed to pure oxygen or nitrogen at different temperatures. All the food models have an initial line width of $\Delta H_{pp} = 0.166 \pm 0.003$ mT which, according to the standard curve, Fig. 3A, corresponds to an atmosphere containing about 21% oxygen. This relatively high oxygen content is noteworthy, since the food models were exposed to high vacuum during freeze-drying. However, the low temperature and the increasing encapsulating effect of the glassy matrix, as the food model dries and the temperature rises, seem to have prevented O_2 from escaping. The line width, ΔH_{pp}, increases with time in the food models exposed to pure

oxygen and, for the food models stored at 60 and 70°C, the permeation process is fast enough to allow the line width to reach an asymptotic value of 0.276 ± 0.003 mT after about 25 days. According to the standard curve (Fig. 3A) this value corresponds to a situation where the encapsulated oil is in equilibrium with the surrounding atmosphere of 100% oxygen. A considerably slower development is observed for food models stored in oxygen at lower temperatures. For example, after 48 days the food models stored at 5 and 45°C only reach non-asymptotic ΔH_{pp} values of 0.18 and 0.25 mT, respectively. Storage in nitrogen at 22°C causes a decrease in the line width and the food models reach a limiting value of 0.154 ± 0.002 mT. This corresponds to an oxygen concentration in the atmosphere of 17.3% O_2, or slightly below, as the standard curve is not linear at these low O_2 concentrations, but the food models are still far from being completely depleted of oxygen. The food model has, in this regard, a high capability of retaining O_2, as the encapsulating properties of the glassy matrix also prevent O_2 from permeating out from the oil phase.

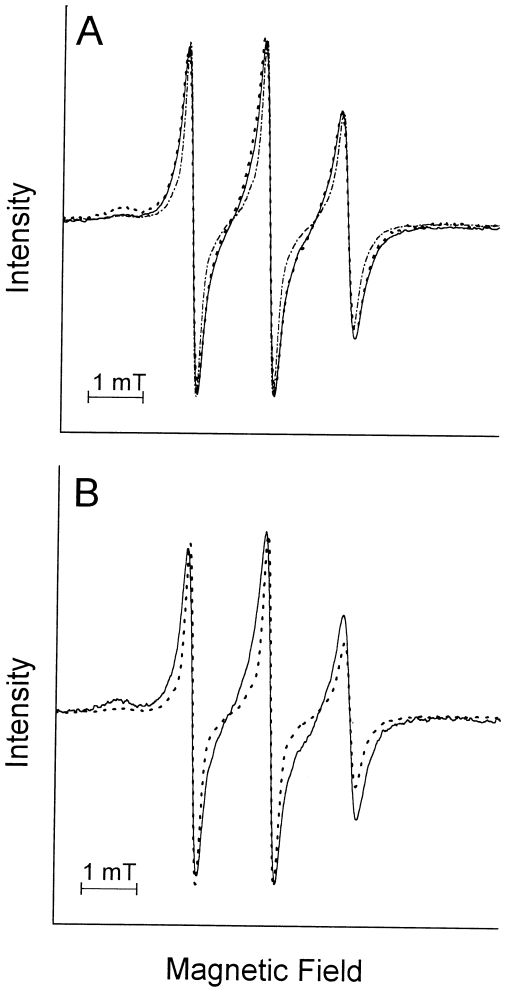

Fig. 4. ESR spectra of food models stored under different conditions. (A) Food models stored at 75°C in 100% O_2 for 1 h (–·–·–), for 1 day (——) and for 30 days (·····). (B) Food models stored at 5°C (·····) and 75°C (——) for 33 days in O_2. The ESR spectra have been normalized by the intensity of the central line.

The food models stored in oxygen at the two highest temperatures (75 and 80°C) show a different and more complex behaviour (cf. Fig. 5C and D). After an initial rapid increase in ΔH_{pp} over the first 6 days, a slow but significant decrease is observed over the next 34 days accompanied by development of a light brown colour of the glassy matrix. A similar decrease in ΔH_{pp} was not seen for the ESR-tubes containing bulk oil stored in the same desiccators, implying that the decrease is related to the specific properties of encapsulated oil stored at high temperatures. MCT oil is characterized as being highly oxidatively stable, as it only contains fully saturated fatty acids. No development of the peroxide value of the oil was recorded after the oil had been stored for 48 days at 5, 22, 37 and 45°C in 100% O_2 or at 22°C in 100% N_2. It can, therefore, be assumed that no oxygen-consuming oxidation has taken place in the oil. Based on the above observations we find it likely that the observed decrease in ΔH_{pp} is caused by an oxidation process in the glassy matrix, consuming oxygen from the encapsulated oil with a rate higher than the replenishment of the permeation process.

The supplementary measurements in interchanged atmospheres showed some seemingly surprising results. When changing the gas from O_2 to N_2 for 10 min for the oxygen incubated food models, a decrease in line width to 0.17–0.21 mT was observed for all temperatures, independently of the line width reached before changing the gas (results not shown). When reintroducing O_2 for 10 min, the line width returned to the level obtained before changing gas. This is surprising since the same food models show slow increases in line width over several days, and also fast decreases on the timescale of minutes, apparently indicating both slow uptake and fast release of oxygen. This apparently contradictory result can be caused by two events. The slow increase may mostly be caused by degradation of the glassy matrix giving rise to a slow release of encapsulated oil to the surface and thereby exposing probes to the atmosphere and allowing a fast release of oxygen when the atmosphere is changed. However, no loss of probe was recorded after washing with hexane after 40 days of storage (results not shown) indicating that the oil remained well encapsulated. Therefore, a more likely explanation is that not all the oil is equally well encapsulated from the start, leaving a minor fraction positioned very close to the surface or present in capillaries that are not easily penetrated by hexane. When the atmosphere is changed to N_2, a situation of an inhomogeneous system arises, similar to the one described in relation to Fig. 3B where a minor part with a low

oxygen concentration may dominate the observed spectrum, resulting in a low peak width. This hypothesis is supported by the fact that no shift in line width was recorded when changing the gas of the nitrogen-incubated samples to O_2. In this case, the influence on the final line width from a minor fraction of broad signals is negligible, as may also be seen from Fig. 3B, from which it is seen that a change in α for low values has little effect on the line width.

3.5. Kinetics and activation parameters for the permeation of oxygen

The similar glass transition temperature and water content of the food model, irrespective of storage temperature, suggest that the observed changes in oxygen permeation result from the temperature-dependence of the oxygen permeation properties of the glassy matrix. In order to interpret the time course of the measured ΔH_{pp} in terms of the temperature dependence of the glassy matrix, it is assumed that the line width, ΔH_{pp}, of the food model system stored at temperature T_i can be expressed as:

$$\Delta H_{pp}(t, T_i) = W(k_i t), \tag{2}$$

where k_i is a material parameter or rate constant assumed to be proportional to the oxygen permeability coefficient of the glassy matrix at the temperature, T_i, $W(x)$ is an a priori unknown and temperature-independent master curve, describing the permeation process in terms of line broadening, and t is the time. This choice of mathematical model using the same master curve $W(x)$ for every temperature is motivated by the fact that all the food models are assumed to have identical geometric properties with respect to distribution of sizes of oil particles and thickness of the glassy matrix covering each of the oil particles. Furthermore, the fact that the

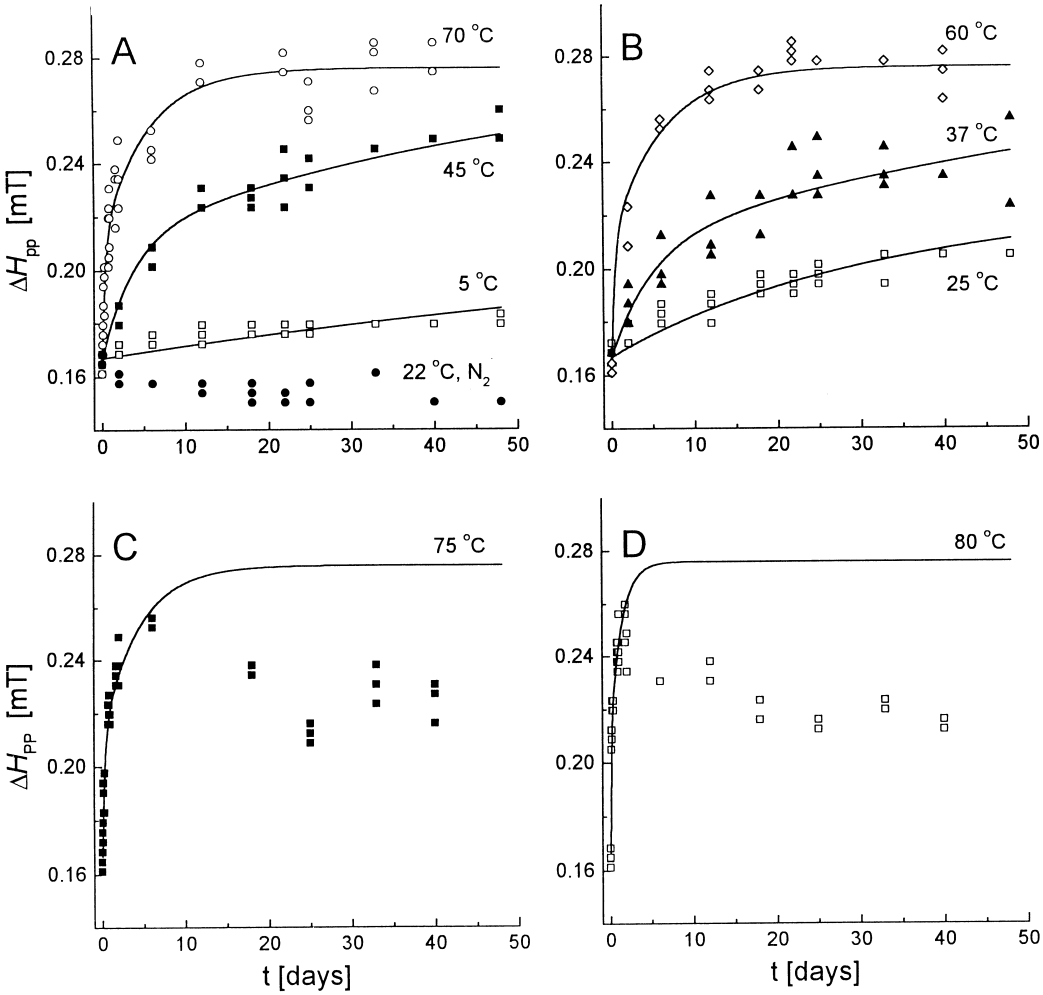

Fig. 5. Time courses of the ESR line width of food models. Measured points and model predictions are shown by symbols and full lines, respectively. (A) Food models stored at 5, 45 and 70°C in 100% O_2 and at 22°C in N_2. (B) Food models stored at 25, 37 and 60°C in O_2. (C) Food models stored at 75°C in O_2. (D) Food models stored at 80°C in O_2. Predictions are based on the double exponential, temperature-independent master curve [cf. Eqs. (2) and (3)], $W(k_i\, t)$, and the temperature-dependent rate constants, k_i, determined for all eight temperatures included in the investigation.

temperature effect of the solubility of oxygen in oil can be neglected also suggests that the asymptotic value of the peak width should be independent of temperature, supporting the mathematical description of Eq. (2). If no other process than permeation is taking place (i.e. no chemical reaction consuming oxygen or redistribution of the glassy matrix above T_g), the course of oxygen saturation of the food model can be described by a combination of a temperature independent master curve, $W(x)$, and a temperature dependent material parameter k_i which controls the timescale of the process as indicated in Eq. (3). The temperature-independent master curve, $W(x)$, is believed to be dependent on specific properties of the food model under study, such as the ratio of poorly encapsulated oil to oil deeply buried in the glassy matrix. The master curve must approach an asymptotic line width $\Delta H_{pp,\infty}$, corresponding to oil saturated with oxygen. We assume that the master curve can be parametrized as a double exponential function:

$$W(x) = \Delta H_{pp,\infty} - A_1 \exp(-x) - A_2 \exp(-B_2 x) \qquad (3)$$

where $\Delta H_{pp,\infty}$, A_1, A_2 and B_2 are positive and temperature independent parameters. Combining Eqs. (2) and (3), and using the eight data sets of the food models stored in oxygen, the eight temperature-dependent k_i values and the four parameters $\Delta H_{pp,\infty}$, A_1, A_2 and B_2, common to all temperatures were determined by a simultaneous non-linear curve fit to all eight data sets. In this way information from all the food models stored in oxygen was used to create the master curve and this procedure ensures that all the rate constants, k_i, correspond to the same kinetic model. Only data from the first two days are used for food models stored at 75 and 80°C (Fig. 5C and D), as an oxygen-consuming process seems to take over at longer storage times. The parameter values obtained by this procedure were $\Delta H_{pp,\infty} = 0.276$ mT, $A_1 = 0.04348$ mT, $A_2 = 0.0658$ mT and $B_2 = 0.0690$ (corresponding to a χ^2 value of 4.45×10^{-5}) and the resulting curves are shown in Fig. 5. It is possible to describe the time-development of ΔH_{pp} at all temperatures using the same function by appropriate scaling [cf. Eq. (2)] of the argument of the master curve $W(x)$. Using a single exponential master curve by fixing A_1 to be 0 mT gave a significantly poorer fit ($\chi^2 = 8.12 \times 10^{-5}$), having too low an asymptotic value of the line width of 0.269 mT. Adding an extra term of $A_3 \exp(-B_3 x)$ did not improve the fit ($\chi^2 = 4.50 \times 10^{-5}$) noticeably as A_3 was determined to have a negligibly small value, in the order of 10^{-7} mT.

Since the rate constants, k_i, are assumed to be proportional to the permeability coefficient of the glassy matrix, the activation energy of the permeation process can be obtained from an Arrhenius plot of the k_i values. Fig. 6 shows the Arrhenius plot corresponding to the double exponential version of $W(x)$. The temperature-dependence of the rate constant is seen to be well described by the Arrhenius equation. An activation energy of 74 ± 6 kJ/mol was found to be independent of the master curve used.

4. Discussion

The ESR line broadening technique appears to be suitable for studying the permeation of oxygen through the glassy matrix of a food model, since the spin probe can be completely incorporated into oil particles, and therefore monitors the oxygen concentration inside the intact food model by non-invasive measurements. The doxyl-substituted stearic acid 16-DSA was found to be useful as a lipophilic spin probe as the long chain of this spin probe hinders translational motion whereas it has only a minor effect on the rotational motion (Hyde & Subczynski, 1989). Thus the contribution of spin exchange between spin probe molecules to the overall line broadening was found to be negligible in the range of nitroxide concentrations from 5 to 217 μM. Any changes in the concentration of the 16-DSA that may take place, either during the preparation of the food models or as a result of the decay of spin probe during the storage of the food models at high temperatures for a long period of time, are, therefore, not expected to contribute to the line broadening of the ESR signals. The relatively high rotational mobility of the spin probe in the oil phase results in an almost isotropic ESR signal where the line broadening effect is easily monitored due to the sharpness of the ESR lines. Furthermore, the similarity between the ESR spectra of 16-DSA in pure MCT oil and in the oil-encapsulating model suggests that the 16-DSA is mainly located in the oil particles, which simplifies the comparison with the spectra of 16-DSA in the pure MCT oil under various oxygen atmospheres.

The use of nitroxide spin probes for ESR oximetry has been developed and used mainly in biological systems where both the temperatures and the duration of the experiments have been lower and shorter than in the present study (Hyde & Subczynski, 1989; Swartz & Glockner, 1989). However, 16-DSA incorporated into the food model was found to be stable when stored at temperatures lower than T_g. At higher temperatures, a significant amount of the spin probe decayed during the experiment, but apart from a loss in intensity, the shape of the ESR spectra were only affected by the oxygen concentration.

An oxygen-consuming process, not involving peroxide formation, took place in the food models stored at 75 and 80°C. A distinct browning of the matrix was observed, probably caused by Maillard reactions

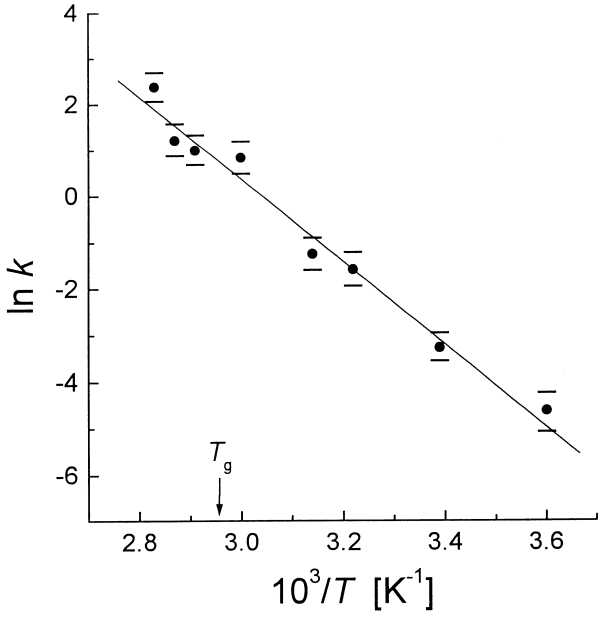

Fig. 6. Arrhenius plot of rate constants, k_i, for oxygen permeation through glassy matrices. The rate constants were evaluated using the same double exponential master curve for all temperatures with a common temperature-dependence incorporated in the two exponential terms.

between the carbohydrate and protein components of the glassy matrix. It is possible that some of the products produced by the Maillard browning reactions are prooxidants initiating oxygen consumption (Wijewickreme & Kitts, 1997). The rate of Maillard browning is known to depend on the glass transition (Bell, 1996; Buera & Karel, 1993; Karmas, Buera & Karel, 1992; Lievonen, Laaksonen & Roos, 1998; Roos & Himberg, 1994), and Maillard browning is largely hindered below T_g due to the low mobility, while the rate of browning increases above T_g, as the viscosity of the system decreases (Bell, 1996; Karmas et al., 1992, Lievonen et al., 1998).

The ESR line widths measured in the food model were inside the range of line widths covered by the standard curve. The initial line widths recorded in the food model were close to the value for an oil in equilibrium with atmospheric air which indicates a high retention of oxygen in the food model despite the evacuation during freeze-drying. This result is of importance to the production of highly oxygen-sensitive products, especially as the results indicate that it is difficult to remove remaining oxygen during the freeze-drying process.

The permeation rate of oxygen through the glassy matrix could be described by the Arrhenius equation during the entire range of storage temperatures, irrespective of the glass transition. The permeation process can, therefore, be regarded as an activated process and, in this respect, the results support the molecular model (Meares, 1954). The activation energy for oxygen permeation in the food model is consistent with activation energies of oxygen permeation in starch films (as estimated from the figures, Arvanitoyannis et al., 1994) and through polyvinyl acetate membranes (Meares, 1954). However, due to the limited range of temperatures above T_g of the food model, the possibility that deviations from the Arrhenius equation or crossover to a higher activation energy exist (Arvanitoyannis, et al., 1994) cannot be entirely eliminated.

Our results confirm that oxygen does permeate glassy matrices at a rate which may be relevant for storage of dehydrated foods, as was also found in the study of oxidation of encapsulated rapeseed oil (Orlien et al., 2000). A complete description of the dissolution of oxygen at the boundaries of the matrix material, and the following diffusion to the surfaces of the oil particles, is a complicated mathematical problem beyond the scope of this paper. However, by using the concepts from food packaging, a simplified theory can be proposed that describes the behaviour of oxygen in food containing encapsulated oil. Each single encapsulated oil particle is treated as a micro package. To a first approximation, the number of oxygen molecules entering the package per unit time would then be proportional to the concentration gradient of oxygen over the "packaging" material covering the oil particle (Robertson, 1993). Thus, if no oxidation is taking place in the oil, the oxygen concentration inside the oil particle should approach the equilibrium value as a first order process, i.e. an exponential increase (or decrease) in oxygen concentration with a time constant inversely proportional to the surface to volume ratio of the particle and the permeability coefficient of the glassy matrix and proportional to the thickness of the "packaging material". If an oxidation process is able to maintain a constant and low oxygen concentration inside the oil particle, the influx of oxygen will be constant and rate limiting, giving rise to zeroth order kinetics of the oxidation process. The constant rate of oxidation will be governed by the same material parameters, namely surface to volume ratio of the particle, the permeability coefficient of the matrix material and the thickness of the encapsulating layers. The present study shows that glassy matrices containing encapsulated oil or fat are complex, since the material contains both, well-encapsulated oil, and oil which can exchange oxygen with the surroundings within a shorter timescale, as seen from the supplementary experiments using interchanged gases. Monitoring the oxygen uptake into a complete ensemble of oil particles by using ESR oximetry is further complicated by the fact that parts of the food model with low concentrations of oxygen dominate the observed ESR line width ΔH_{pp}. On the basis of these considerations, the uptake of oxygen into a multiple of differently-encapsulated oil particles is unlikely to be a simple first order process, supporting the finding that the time course of the ΔH_{pp} could not be described by a single exponential master curve.

As oxygen is shown to permeate the glassy matrix, oil encapsulated in the food models may not be completely protected from oxidation, even though the integrity of the glassy matrix is preserved. Studies of oxidation of encapsulated oil show that the process proceeds as a zeroth order process, indicating that permeation of oxygen is the limiting step (Anandaraman & Reineccius, 1986; Orlien et al., 2000). Our results indicate that, in such systems, some oil particles may oxidize rapidly and some more slowly, due to inhomogeneity in the degree of encapsulation. The observed constant rate of oxidation should, therefore, be regarded as an average rate of all the individual zeroth order processes taking place in each of the oil particles. As oxidation of encapsulated oil is controlled by the permeation process, we expect the oxidation process to follow the same temperature dependency as the permeation process. The finding of a large activation energy, 74 kJ/mol, for the permeation process in the present food model, suggests that temperature is important for the protective properties of glass encapsulation.

5. Conclusion

Oximetry, based on the broadening of ESR-lines in the presence of oxygen, has been developed to follow the permeation of oxygen through a glassy matrix encapsulating-oil containing the spin probe 16-DSA. The permeation of oxygen increased with the temperature, and a kinetic model could be established from which the energy of activation for oxygen permeation was derived. While the numerical values of the kinetic parameters used to describe the oxygen permeation must be considered valid only for the actual food model with its specific size-distribution, the energy of activation is of more general relevance since it describes the process of permeation for this type of food model, irrespective of the actual size-distribution. The method should allow non-invasive determination of oxygen depletion in dried food and will be tested on other such products sensitive to oxidative deterioration.

Acknowledgements

This work was funded by the FØTEK program through LMC-Centre for Advanced Food Studies as the project "Phase Transitions in Food". Svend E. Knudsen is thanked for skilful technical assistance.

References

Afeworki, M., Miller, N. R., Devasahayam, N., Cook, J., Mitchell, J. B., Subramanian, S., & Krishna, M. C. (1998). Preparation and EPR studies of lithium phthalocyanine radical as an oxymetric probe. *Free Radical Biology & Medicine, 25*, 72–78.

Anandamaram, S., & Reineccius, G. A. (1986). Stability of encapsulated orange peel oil. *Food Technology*, *November*, 88–92.

Andersen, A. B., Fog-Petersen, M. S., Larsen, H., & Skibsted, L. H. (1999). Storage stability of freeze-dried starter cultures (*Streptococcus thermophilus*) as related to physical state of freezing matrix. *Lebensmittel Wissenschaft und Technologie*, *32*, 540–547

Arvanitoyannis, I., Kalichevsky, M. T., & Blanshard, J. M. V. (1994). Study of diffusion and permeation of gases in undrawn and uniaxially drawn films made from potato and rice starch conditioned at different relative humidities. *Carbohydrate Polymers, 24*, 1–15.

Bell, L. N. (1996). Kinetics of non-enzymatic browning in amorphous solid systems: distinguishing the effects of water activity and the glass transition. *Food Research International, 28*, 591–597.

Buera, M. d. P., & Karel, M. (1993). Application of the WLF equation to describe the combined effects of moisture and temperature on nonenzymatic browning rates in food systems. *Journal of Food Processing and Preservation, 17*, 31–45.

Hyde, J. S., & Subczynski, W. K. (1989). Spin-label oximetry. In L. J. Berliner, & J. Reuben, *Biological magnetic resonance, vol. 8* (pp. 399–425). New York: Plenum Press.

IDF standard 74A (1991). International Dairy Federation, Bruxelles.

Imagi, J., Muraya, K., Yamashita, D., Adachi, S., & Matsuno, R. (1992). Retarded oxidation of liquid lipids entrapped in matrices of saccharides or proteins. *Bioscience Biotechnology and Biochemistry, 56*, 1236–1240.

Inoue, M., Utsumi, H., & Kirino, Y. (1994). A comparative ESR study of some paramagnetic materials as probes for the noninvasive measurement of dissolved oxygen in biological systems. *Chemical & Pharmaceutical Bulletin, 42*, 2346–2348.

Karmas, R., Buera, M. P., & Karel, M. (1992). Effect of glass transition on rates of nonenzymatic browning in food systems. *Journal of Agricultural and Food Chemistry, 40*, 873–879.

Labrousse, S., Roos, Y., & Karel, M. (1992). Collapse and Crystallization in Amorphous Matrices with Encapsulated Compounds. *Sciences des Aliments, 12*, 757–769.

Lievonen, S. M., Laaksonen, T. J., & Roos, Y. (1998). Glass transition and reaction rates: nonenzymatic browning in glassy and liquid systems. *Journal of Agricultural and Food Chemistry, 46*, 2778–2784.

Meares, P. (1954). The diffusion of gases through polyvinyl acetate. *Journal of the American Chemical Society, 76*, 3415–3422.

Morse, P. D., & Smirnov, A. I. (1995). Simultaneous ESR measurements of the kinetics of oxygen consumption and spin label reduction by mammalian cells. *Magnetic Resonance in Chemistry, 33*, S46–S52.

Orlien, P. V., Andersen, A. B., Sinkko, T., & Skibsted, L. H. (2000). Hydroxide formation in rapeseed oil encapsulated in a glassy food model system as influenced by hydrophilic and lipophilic radicals. *Food Chemistry, 68*, 191–199.

Robertson, G. L. (1993). *Food packaging: principle and practice*. New York: Marcel Dekker.

Roos, Y. H., & Himberg, M.-J. (1994). Nonenzymatic browning behaviour as related to glass transition of a food model at chilling temperature. *Journal of Agricultural Food Chemistry, 42*, 893–898.

Sun, W. Q., Leopold, A. C., Crowe, L. M., & Crowe, J. H. (1996). Stability of dry liposomes in sugar glasses. *Biophysical Journal, 70*, 1769–1776.

Swartz, H. M., & Glockner, J. F. (1989). Measurements of the concentration of oxygen in biological systems using EPR techniques. In A. J. Hoff, *Advanced EPR. Application in biology and biochemistry* (pp. 753–784). Amsterdam: Elsevier.

Wijewickreme, A. N., & Kitts, D. D. (1997). Influence of reaction conditions on the oxidative behavior of model Maillard reaction products. *Journal of Agricultural and Food Chemistry, 45*, 4571–4576.